Supporting Information

Photochemical Action Plots Evidence UV-promoted Radical Ring-Opening Polymerisation of Cyclic Ketene Acetals

Till Meissner,[a,b,c] Peter Friedel, [a] Joshua A. Carroll, [c] Christopher Barner-Kowollik *[c,d] and Jens Gaitzsch *[a]

[a.] *Leibniz-Institut für Polymerforschung Dresden e.V., Hohe Strasse 6, 01069 Dresden, Saxony, Germany. Email: gaitzsch@ipfdd.de*
[b.] *Faculty of Chemistry and Food Chemistry, Organic Chemistry of Polymers, Technische Unversität Dresden, Bergstrasse 66, 01059 Dresden, Saxony, Germany.*
[c.] *School of Chemistry and Physics, Queensland University of Technology (QUT), 2 George Street, 4000 Brisbane, QLD (Australia). Email: christopher.barnerkowollik@qut.edu.au*
[d.] *Institute of Nanotechnology (INT), Karlsruhe Institute of Technology (KIT), Herrmann-von-Helmholtz-Platz 1, 76344 Eggenstein-Leopoldshafen (Germany)*

Table of Contents

1 Materials and Methods 1

1.1 Spectroscopy 1

1.1.1 Laser 1

1.1.2 UV/Vis spectroscopy 1

1.1.3 NMR spectroscopy 1

1.2 Chromatography 2

1.3 Computational methodologies 2

2 Experimentals 3

2.1 MTC synthesis 3

2.2 Characterisation of reaction mixture 3

2.3 General experimental laser setup[12] 5

2.4 Determination of quartz laser vial transmission 6

2.5 Laser experiments MTC/AIBN 6

2.6 Reference experiments MMA/AIBN 9

2.7 UV/Vis experiments 12

2.8 Computational studies 15

3 References 17

1 Materials and Methods

Unless stated otherwise, all chemicals were used as received without further purification. THF, $CHCl_3$ and MeOH were purchased from Thermo Fisher Scientific. Chloroacetaldehyde dimethyl acetal (CADMA), *tert*-butanol (^{t}BuOH), potassium *tert*-butoxide (^{t}BuOK), Dowex® 50WX8, 2,2'-azobis(2-methyl-propionitrile) (AIBN) and methyl methacrylate (MMA) were purchased from Sigma Aldrich. ^{t}BuOK was stored under an anhydrous atmosphere (desiccator). AIBN was recrystallised from MeOH prior to use. ^{t}BuOH was deoxygenised via multiple freeze-pump-thaw cycles as well as degassed with argon and stored in the fridge in a Schlenk-flask under an argon atmosphere. The investigated CKA 2-methylene-1,3,6-trioxocane (MTC) was synthesised following a literature-known protocol and stored in a Schlenk-flask under argon at -20 °C.[1, 2] Deuterated solvents for NMR spectroscopy were purchased at Cambridge Isotope Laboratories. Concerning reactions were performed under inert and moisture free conditions, flasks and other glassware were evacuated while heated, followed by flooding with argon (99.999% purity).

1.1 Spectroscopy

1.1.1 Laser

For the action plot (AP) measurements, the irradiation sources were monochromatic optical parametric oscillators (OPOs), which emit five nanosecond pulses at either 20 Hz tunable from 210 nm up to 2400 nm (Opotek Opolette 355) or 100 Hz tunable from 240 nm up to 580 nm (Innolas Spitlight EVO), both with a bandwidth of 4-6 cm^{-1}.

1.1.2 UV/Vis spectroscopy

UV/Vis spectra were recorded using either a 1 cm (Starna) or a 2 mm optical path length (OPL) quartz glass cuvette with a sample volume of 2 mL or 400 µL at 20 °C on a Cary 100 Scan UV/Vis spectrometer (Varian), respectively.

UV/Vis absorbance was also measured utilising a 1 cm or a 2 mm OPL quartz glass cuvette with a sample volume of 400 µL at room temperature (RT) on a Specord 210 Plus UV/Vis spectrometer (Analytik Jena), respectively. The spectral band width was a 1 nm slit with a 10 mm cell older which was temperature controllable. The integration time amounts to 0.02 s with a scanning speed of 5 nm/s. A cooled double detection (CDD) system was employed.

1.1.3 NMR spectroscopy

^{1}H-NMR spectroscopic data were recorded on a Bruker Avance 600 MHz spectrometer at ambient temperature. The chemical shifts are reported in δ units, parts per million (ppm) downfield from TMS. Deuterated chloroform ($CDCl_3$) was used as solvent and reference (δ(^{1}H) = 7.26 ppm).

Additionally, ^{1}H-NMR measurements were performed using a Bruker Advance III 500 spectrometer operating at 500.13 MHz for ^{1}H. The measurements were carried out at 30 °C using standard pulse sequences of the TopSpin 3.2 software package (Bruker Biospin).

1.2 Chromatography

Size exclusion chromatography (SEC)

The SEC measurements were conducted on a *PSS* SECurity^{2} system consisting of a *PSS* SECurity Degasser, *PSS* SECurity TCC6000 Column Oven (35 °C), *PSS* SDV Column Set (8x150 mm 5 µm Precolumn, 8x300 mm 5 µm Analytical Columns, 100000 Å, 1000 Å and 100 Å) and an *Agilent* 1260 Infinity Isocratic Pump, *Agilent* 1260 Infinity Standard Autosampler, *Agilent* 1260 Infinity Diode Array and Multiple Wavelength Detector (A: 254 nm, B: 360 nm), *Agilent* 1260 Infinity Refractive Index Detector (35 °C). HPLC grade THF, stabilised with BHT, is used as eluent at a flow rate of 1 mL·min^{-1}. Narrow disperse linear poly(styrene) (M_n: 266 g mol^{-1} to 2.52x10^{6} g mol^{-1}) and poly(methyl methacrylate) (M_n: 202 g mol^{-1} to 2.2x10^{6} g mol^{-1}) standards (*PSS* ReadyCal) were used as calibrants. All samples were passed over 0.22 µm PTFE membrane filters. Molecular weight and dispersity analyses were performed in *PSS* WinGPC UniChrom software (version 8.2).

1.3 Computational methodologies

Ab-initio calculations

Ab-initio calculations were performed in order to optimise the geometry and determine the atomic charges by minimising the corresponding Hartree-Fock energy and to determine the atomic charges (Mullikan[3] and Lowdin[4] method) applying the software package GAMESS[5] using the basis set STO-6G.[6] In exceptional cases, the Sapporo-(PK)-AnZP basis set family was applied.[7] Further ab-initio calculations were carried out using basis sets from the Jensen[8] (PC-SEG-0 and APC-SEG-0) as well as the Dunning family, entailing CCD, ACCD, and KTZV as basis sets.[9-11]

Single molecular calculations

These ab-initio calculations were applied in detail to the structure of the 2-ethyl-1,3,6-trioxocane radical using a multiplicity of 2 for the purpose of optimising the molecular geometry.

Transition moment calculations

The GAMESS program packages allow also for the calculation of transition moments which were applied to the corresponding optimised molecular structures.[5]

2 Experimentals

2.1 MTC synthesis

The investigated CKA MTC was synthesised according to a previously published procedure.[1, 2] The synthetical sequence is displayed in the following and discussed briefly (**Scheme S1**).

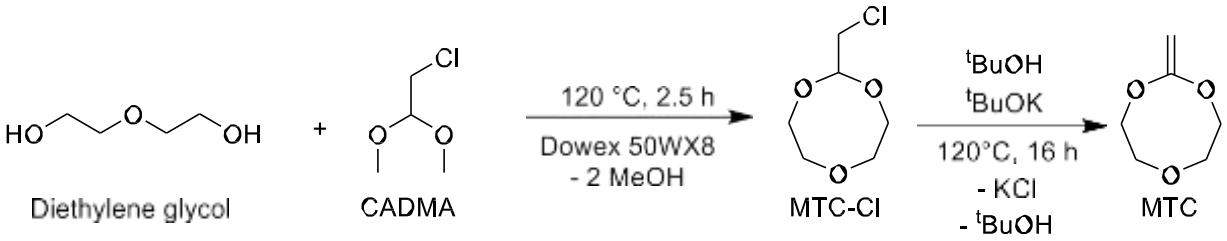

***Scheme S1**. MTC synthesis entailing transacetalisation of CADMA via an acidic resin, yielding the halogenated acetalic MTC-Cl and subsequent elimination reaction with ^{t}BuOK towards the monomer MTC.*

In the first step, 201.2 mL of CADMA (220.1 g, 1.77 mol, 1.14 eq.) were mixed with 146.9 mL (164.5 g, 1.55 mol, 1 eq.) diethylene glycol and 2.44 g Dowex 50WX8 in a two-necked flask. After equipping with a Claisen condensation bridge attached to second two-necked flask, the reaction mixture was heated to 120 °C whilst applying a gentle N_2 flow for 2.5 h to remove the generated MeOH. Subsequently, the reaction mixture was cooled to RT. The leftover CADMA was distilled off under reduced pressure (0.15 mbar, 140 °C). After recondensation, MTC-Cl (200 g, 1.2 mol, 78%) was obtained as a colourless, crystalline solid.

The second reaction step comprised the elimination towards the exocyclic double bond yielding the monomer MTC. Therefore, 80 g (482 mmol, 1 eq.) of MTC-Cl and 65 g (580 mmol, 1.2 eq.) of ^{t}BuOK were dissolved in 280 mL ^{t}BuOH while stirring. The reaction mixture was further stirred for 15 min while bubbled with N_2. The solution was transferred into a pressure flask and heated to 120 °C for 16 h. After cooling down to RT, diethyl ether was added and the suspension was filtrated and the solid residue washed with diethyl ether multiple times. After removal of the solvent *in vacuo*, the product was distilled under reduced pressure (35 mbar, 82 °C) multiple times to obtain sufficiently (>99.5%) pure CKA monomer MTC. Eventually, MTC was collected as a colourless and water-sensitive liquid in a quantity of 15 ml (26%).

^{1}H-NMR (600 MHz, $CDCl_3$, ppm): 3.67 (s, 2H, H9), 3.76-3.79 (m, 4H, H3+5), 4.04-4.09 (m, 4H, H2+6).

2.2 Characterisation of reaction mixture

The determination of monomer conversion (MTC) and density of branches (DB) of the obtained PMTC was conducted via ^{1}H-NMR spectroscopy (**Scheme S2**).

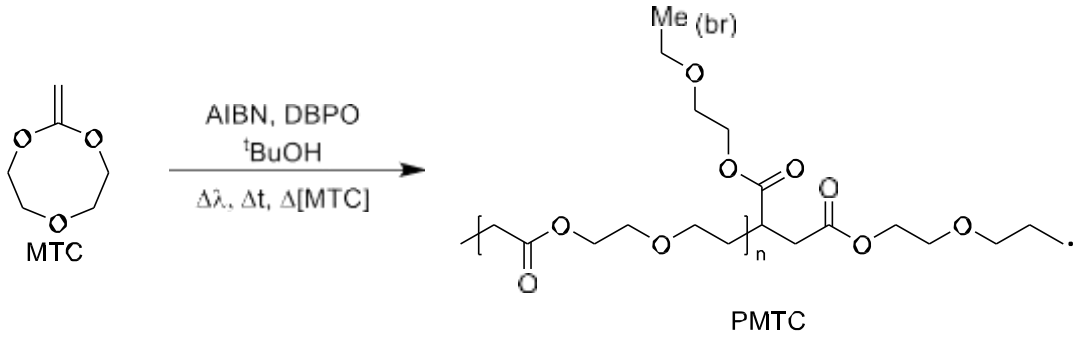

***Scheme S2**. General reaction scheme of RROP of MTC with varied reaction parameters and resulting PMTC structure showcasing side branches.*

For quantifying the depleted MTC, the integral intensity of the methylene groups of the remaining MTC ring protons was placed in relation to the growing integral intensity of a methylene group resonance associated with the formed polymer's polyester backbone, such as H6 or H24 (**Figure S1**).

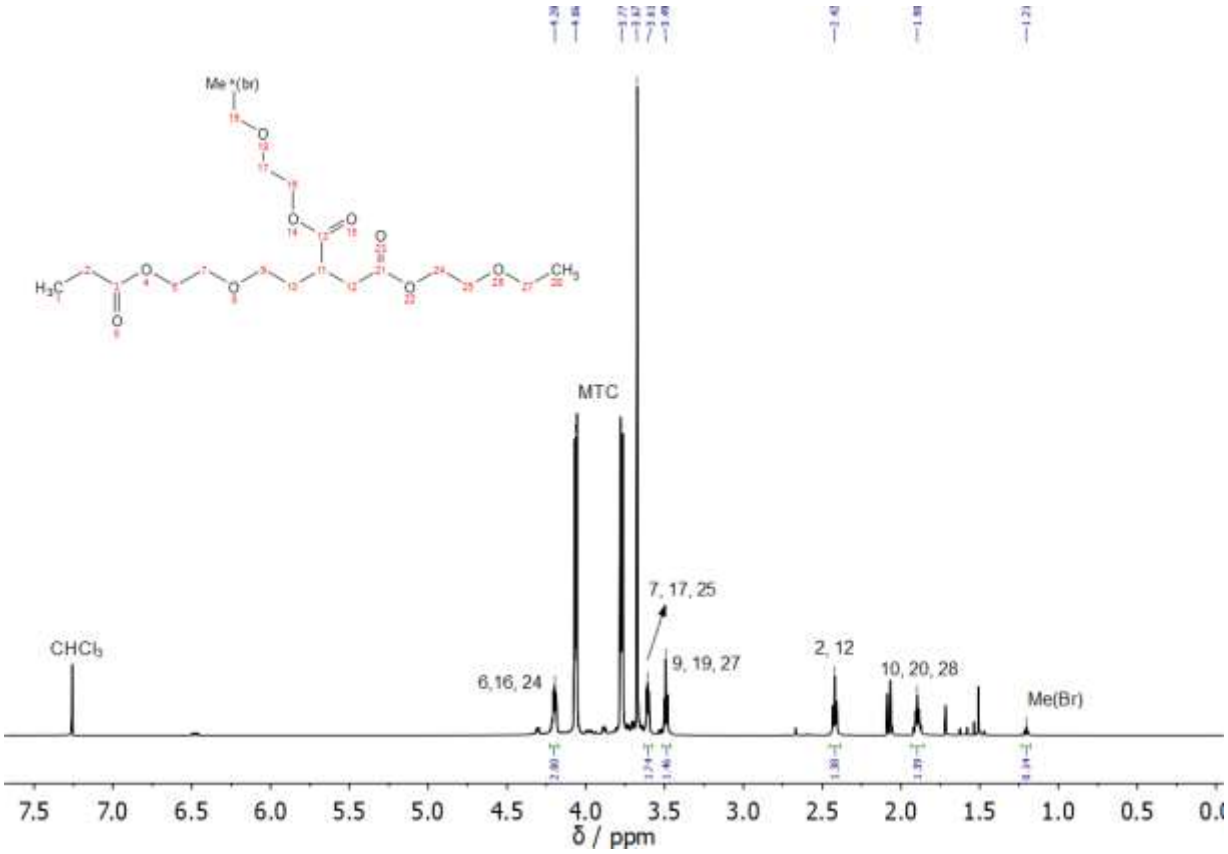

***Figure S1**. [1]H-NMR spectrum of the crude reaction mixture containing MTC, AIBN, and PMTC with assigned protons necessary for monomer conversion and DB determination.*

For the determination of the DB, the following equation 1 was applied in accordance with the literature.[12]

$$DB\ [\%] = \frac{2 * I(Me(br))}{3 * I(H6{,}24)} * 100\% \qquad (1)$$

The integrated resonance of the introduced methyl branch in the side chain (Me(br)) of the growing polymer was put in relation to the intensity of a methylene group of the PMTC backbone unsusceptible to proton abstraction (H6 or H24) to yield an averaged DB.

2.3 General experimental laser setup[12]

The general laser setup comprises an optical parametric oscillator (OPO), a polariser for adjusting the delivered energy at the end of the setup, several lenses to expand and focus the laser beam, a prism to center the beam onto the hole of the sample holder where either a glass or a quartz cuvette – depending on the employed wavelength – was immersed and an energy meter comprising a sensor, which is tethered to a processing unit for real time evaluation of the energy output (**Scheme S3**).

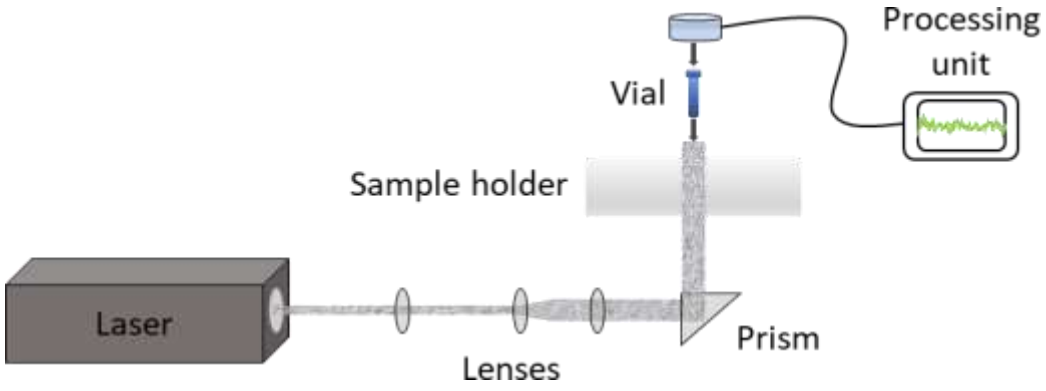

***Scheme S3**. General experimental laser setup comprising a monochromatic optical parametric oscillator (OPO) as monochromatic light source, optical lenses, prism, laser vial with the sample immersed in a holder as well as an energy meter with an attached evaluation unit. Adapted and modified from* Irshadeen *et al.*[12]

As outlined by Irshadeen *et al.*, an equal photon flux (N_p) applied to the reaction mixture for different wavelengths is mandatory in order to achieve comparability.[12] The dose of radiation stemming from a pulsed laser system can be deduced by the following equation (1).

$$N_p = \frac{E_{pulse} f_{rep} \lambda t}{hc[\frac{T_\lambda}{100}]} \qquad (1)$$

With h and c as Planck's constant and the vacuum speed of light, respectively, as natural constants and f_{rep} as the laser's repetition rate as well as material-specific wavelength-dependent transmission T_λ, the reaction time t (which was set to a certain value beforehand) and the energy of each laser pulse (E_{pulse}) can be adjusted to ensure a congruent number of photons.

2.4 Determination of quartz laser vial transmission

For experiments conducted at wavelengths below 290 nm, quartz laser vials were used instead of glass ones due to their enhanced transmission in this spectral regime. To determine their exact transmission values at specific wavelengths, an established procedure by Menzel *et al.* was employed to ascertain a constant photon flux (**Figure S2**).[13]

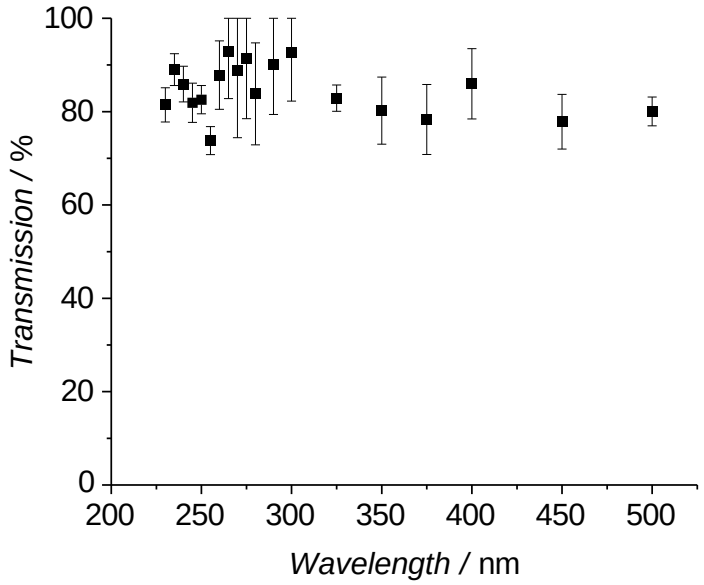

***Figure S2**. Experimentally determined quartz glass laser vial transmissions as well as their deviation bars in dependence of the utilised wavelength, following a protocol established by* Menzel *et al.*[13]

2.5 Laser experiments MTC/AIBN

The sample preparation for a laser experiment follows the same procedure for every individual sample throughout this experimental work.

Sample preparation

A 0.8 mL glass/quartz vial was crimped with a lid with an integrated septum and heated under vacuum once. The vial was flushed with argon and allowed to cool to RT. Subsequently, 1 mol% of AIBN (2.1 mg, with respect to V(MTC)) was weighed in a SEC vial and mixed with 150 µL of ^{t}BuOH and MTC to obtain 300 µL of a 1:1 vol% diluted 4.2 M MTC containing solution. After complete dissolution of the initiator, the mixture was transferred into the prepared laser vial via syringe and bubbled with argon gas for 5 min. Subsequently, the crimped laser vial was sealed with another septum placed on top upside down.

Laser irradiation

Prior to the experiments, the power supply and cooling for the laser was turned on for approximately 1 h and subsequently was operated at the first wavelength for another 30-45 min to reach an output energy equilibrium. Prior to immersion of the laser vial into the sample holder, the collimated laser beam was centered on the hole within the sample holder and the energy was monitored via energy meter and adjusted to ensure an equally applied photon flux to the probe for every individual wavelength. The laser pulse energy was also measured after the experiments to monitor the fluctuation of the energy output of the laser over time. The exact energy at each specific wavelength was calculated depending on the glass vial transmission as well as the photon energy adapting the method developed by Irshadeen *et al.*[12] When everything was set up, the degassed reaction mixture was placed in the sample holder and irradiated at the desired wavelength for 15 min.

According to previously described equation (1), the number of photons over the course of 15 min was set to $N_p = 3.25 * 10^{18}$ for all samples. The calculated laser energy values for recording the MTC/AIBN AP are depicted in the following (**Table S1**).

***Table S1**. Experimentally determined conversion of MTC in dependence of the employed wavelength of the laser light and its corresponding energy for an equal number of photons.*

Wavelength / nm	*Laser energy /* µJ	*Conversion /* %
235	172	0.4
250	174	3.8
260	157	7
270	150	8.3
275	143	9.5
280	153	8.5
285	145	6.4
290	294	6.5
308	180	6.5
320	154	8.7
340	132	8.3
360	120	8.7
380	112	8.3
400	106	3
420	100	0.5

After the set reaction time, the vial was removed from the sample holder and the polymerisation quenched via exposure to ambient atmosphere as well as cooled in an ice bath. The quenched reaction

solution was analyzed via ^{1}H-NMR spectroscopy in order to determine the wavelength-dependent MTC conversion (**Figure S3**).

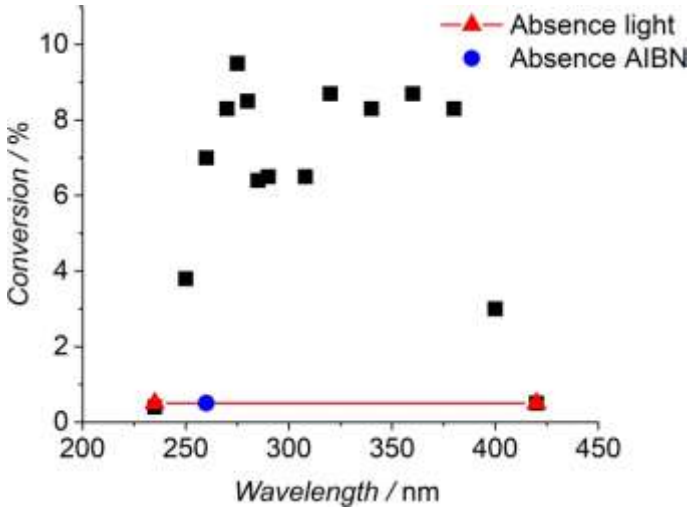

***Figure S3**. AP showcasing wavelength-resolved conversion of MTC in ^{t}BuOH in a 1:1 ratio with 1 mol% of AIBN (black) as well as control samples reacted under absence of incident light (red) and radical initiator AIBN (blue).*

For the kinetic measurements at either 275 or 350 nm, their corresponding polymerisation rate coefficients k_{pol} were calculated via plotting $\ln(c_0/c)$ against the irradiation time and subsequent linear regression, as depicted in the following exemplification (**Figure S4**).

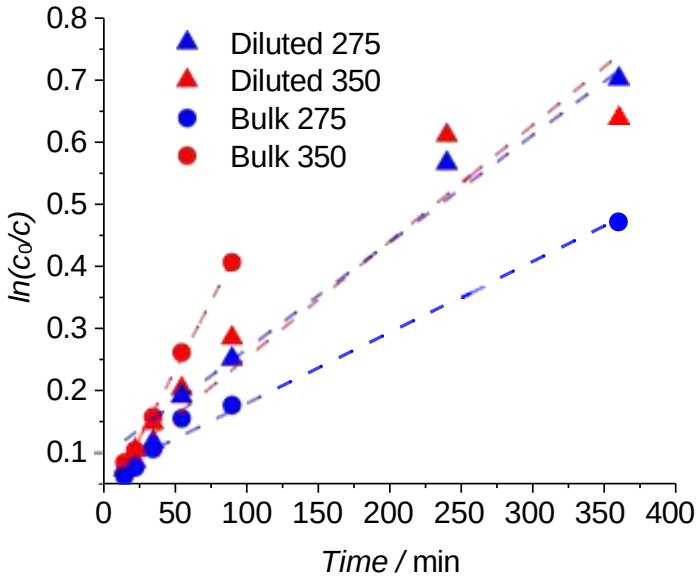

***Figure S4**. Ln(c_0/c) vs. time plot with corresponding regression curves for k_{pol} calculation.*

The determined k_{pol} values were determined from the slopes of the regression curves and are listed together with their errors in the following (**Table S2**).

***Table S2**. Determined k_{pol} values for the performed kinetics and their corresponding deviations.*

Measurement series	k_{pol} / L (mol s)$^{-1}$
Diluted 275 nm	$1.9 \cdot 10^{-3} \pm 1 \cdot 10^{-4}$
Diluted 350 nm	$1.7 \cdot 10^{-3} \pm 2 \cdot 10^{-4}$
Bulk 275 nm	$1.1 \cdot 10^{-3} \pm 6 \cdot 10^{-5}$
Bulk 350 nm	$4.4 \cdot 10^{-3} \pm 1 \cdot 10^{-4}$

For SEC characterisation, the laser vials were decrimped and the volatile compounds were evaporated over night at RT in a vacuum drying oven. Subsequently, a sample of the viscous residue was dissolved in THF. THF-SEC measurements yielded the following elution curves (**Figure S5**A). From the comparison with a previously PMMA standards, the corresponding molecular weights were obtained from the elution curves and were plotted against the monomer conversion (**Figure S5**B).

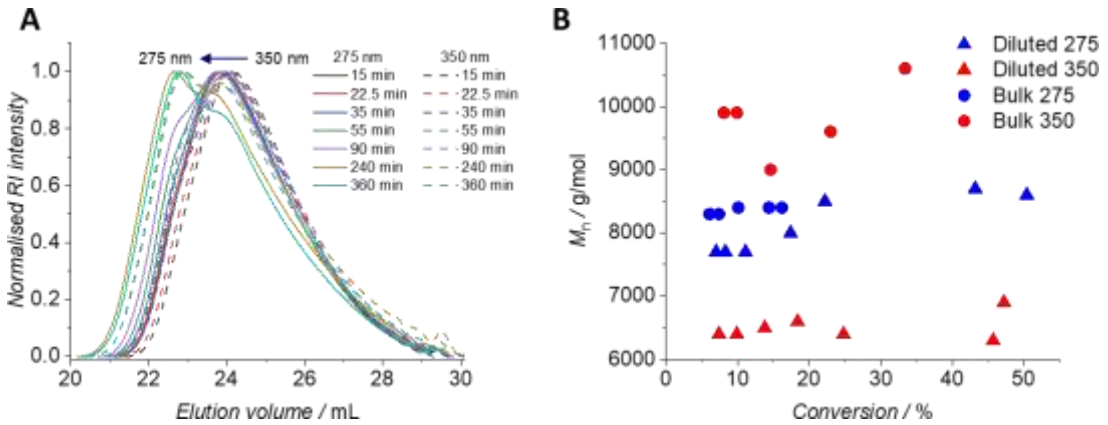

***Figure S5**. (A) Elution curves measured for 275 (bold) and 350 nm (dashed) diluted kinetics and (B) comprehensive relatively determined M_n vs. conversion development for $\Delta[MTC]_0$ at 275 and 350 nm.*

2.6 Reference experiments MMA/AIBN

Sample preparation

A reference AP utilising MMA/AIBN was recorded under identical conditions as reported in chapter 2.5. The sample preparation and composition were kept the same, while for 150 µL of MMA 2.3 mg of AIBN were employed as 1 mol%. Prior to mixing with ^{t}BuOH and AIBN, MMA was activated via running 2-3 mL over a thick layer of neutral activated aluminum oxide in a syringe. For the reference experiments utilising different initial MMA concentrations, the following sample compositions were generated (**Table S3**).

***Table S3**. Sample compositions for reference experiments comprising varying $[MMA]_0$ mixed with a constant amount of AIBN.*

$[MMA]_0$ / mol L^{-1}	*V(MMA)* / µL	*V(^{t}BuOH)* / µL	*m(AIBN)* / mg
4.7	150	150	2.3
1	32	268	2.3
0.5	16	284	2.3
0.1	3.2	296.8	2.3

As a result, the lower the initial MMA concentration, the lower the absorbance of the reaction mixture below 300 nm.

Laser irradiation

The laser experiments with MMA/AIBN as reference system were conducted as described in chapter 2.5 for MTC/AIBN with the following wavelength-resolved conversion (**Table S4**).

***Table S4.** Experimentally determined conversion of MMA in dependence of the employed wavelength of the laser light and its corresponding energy for an equal number of photons.*

Wavelength / nm	*Laser energy* / µJ	*Conversion* / %
235	172	0
260	157	0
290	294	0
305	190	3.5
308	180	5.9
320	154	6.5
340	132	6
360	120	6.8
380	112	5.4
400	106	2
420	100	0

The resulting MMA conversion in dependence of the utilised wavelength is mapped in the following exemplification (**Figure S6**).

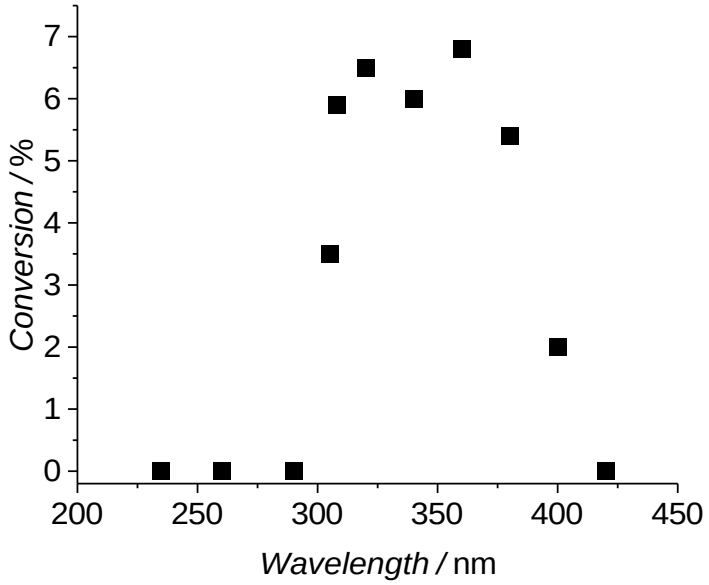

***Figure S6**. AP assessing the wavelength-resolved conversion of MMA in 1:1 dilution utilising 1 mol% of AIBN at RT.*

To further underpin the absence of PMMA formation at 275 nm out of photolytic AIBN decay generating radicals, a serial dilution of MMA was conducted with a consistent amount of AIBN (refer to **Table S3**). Irradiation took place for 15 min at RT and potential PMMA formation was monitored via ^{1}H-NMR spectroscopy (**Figure S7**).

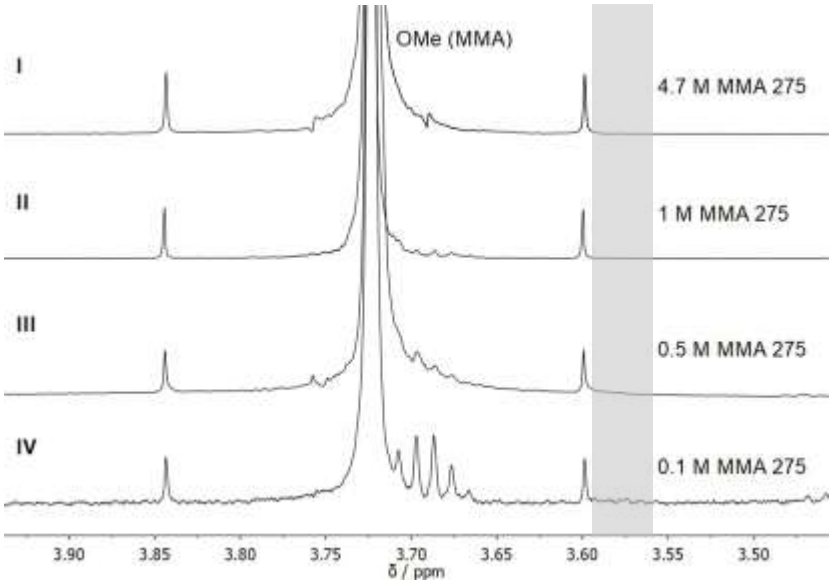

***Figure S7**. ^{1}H-NMR spectra for different $[MMA]_0$ at 275 nm indicating the absence of PMMA formation.*

Additionally, a reaction mixture containing 0.5 M MMA in ^{t}BuOH was exposed for the same period of time to either 275 or 350 nm in order to clearly showcase the wavelength-dependent cleavage of AIBN capable of initiating radical polymerisation of MMA (**Figure S8**A).

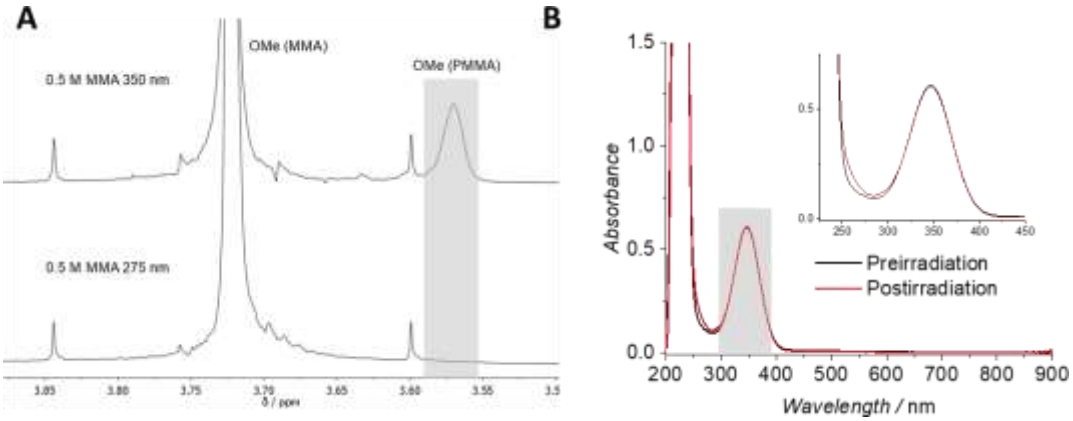

***Figure S8**. (A) ^{1}H-NMR spectra of 0.5 M MMA with 1 mol% AIBN irradiated at either 275 (bottom) or 350 nm (top), underpinning the UV-initiated decay of AIBN at 350 nm by PMMA formation and (B) UV/Vis spectra of methyl isobutyrate (equivalent to 0.5 M MMA) in ^{t}BuOH with AIBN prior to and after UV exposure at 275 nm showcasing the augmented area of the characteristic AIBN band at 350 nm.*

Further, UV/Vis spectra prior to and after irradiation at 275 nm were assessed of reaction mixtures comprising methyl isobutyrate as an MMA analogue, ^{t}BuOH, and AIBN (**Figure S8**B). In order to avoid volume losses through transfer, irradiation directly took place in a quartz UV/Vis cuvette with a transparent bottom. Also, the aluminum sample holder had to be replaced by a 3D-printed plastic inlay with a fitting bezel. Besides, the monochromatic laser beam had to be expanded onto the enlarged surface area of the quartz UV/Vis cuvette.

2.7 UV/Vis experiments

As for the standard UV/Vis experiments at RT, a 2 mm OPL quartz glass cuvette was used with a total sample volume of 0.4 mL comprising 0.2 mL of either MTC or MMA and 0.2 mL ^{t}BuOH with a constant mass of AIBN (1 mol%; 2.8 and 3.1 mg for MTC and MMA, respectively). After mixing in a separate SEC vial, the solution was degassed with argon for 5 min. Subsequently, the cuvette was sealed and placed in the UV/Vis spectrometer complying with the parameters mentioned in chapter 1.1.2. A serial dilution of different initial MMA concentrations was subjected to UV/Vis spectroscopy to determine their inherent absorbances at 275 nm (**Table S5**+**Figure S9**).

***Table S5**. Sample compositions for reference experiments comprising varying $[MMA]_0$ mixed with a constant amount of AIBN.*

$[MMA]_0$ / mol L^{-1}	*V(MMA)* / µL	*V(*^{t}*BuOH)* / µL	*M(AIBN)* / mg
4.7	200	200	3.1
1	42.6	357.4	3.1
0.5	21.3	378.7	3.1
0.1	4.3	395.7	3.1

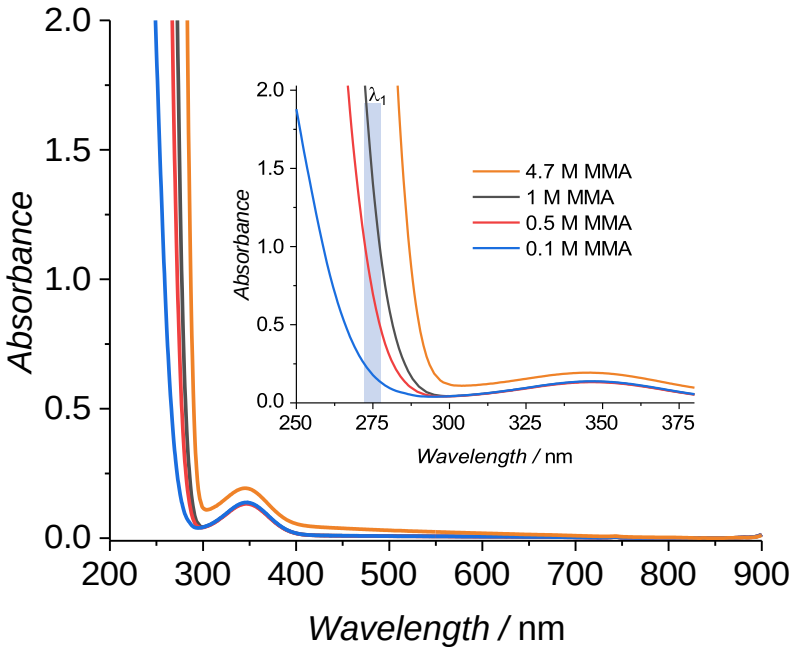

***Figure S9**. UV/Vis spectra of different $[MMA]_0$ in ^{t}BuOH with a constant amount of AIBN together with the augmented area showcasing the absorbance of light with λ_1 = 275 nm.*

For the coupled laser/UV/Vis experiments, a 1 cm OPL quartz cuvette with 2 mL of sample volume was used. The reaction mixture comprised 0.107 mL methyl isobutyrate, 1.893 mL ^{t}BuOH and 15.33 mg AIBN identical to a 0.5 M MMA experiment with 1 mol% of AIBN. Prior to the experiment, the solution was degassed with argon for 5 min and the cuvette sealed with a screw lid. The UV/Vis absorptivity was measured before and after irradiation with UV light of 275 nm (**Figure S8**B). An UV/Vis spectrum of pure 1 mol% AIBN with respect to a hypothetically used monomer with a volume of 200 µL in ^{t}BuOH to determine its absorbance particularly at 275 nm is depicted in the following (**Figure S10**).

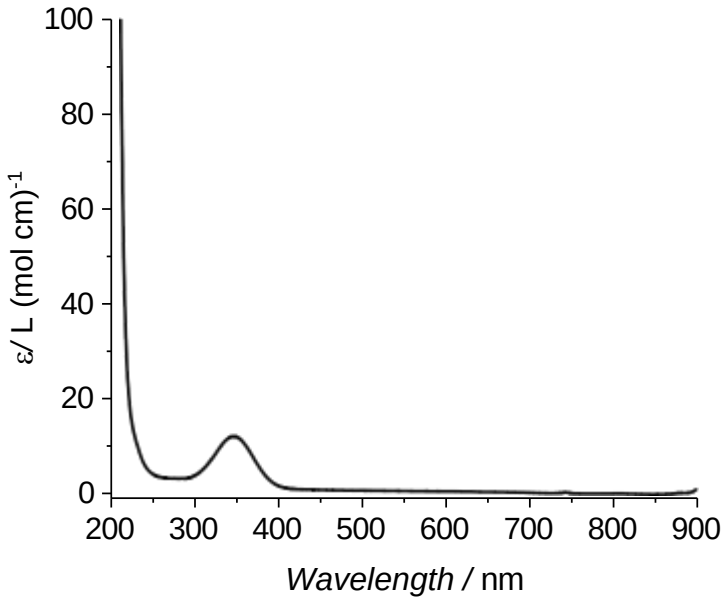

***Figure S10**. UV/Vis spectrum of pure AIBN in ^{t}BuOH with a concentration of 61 mmol L^{-1} in a 0.2 cm optical path length quartz cuvette.*

In order to determine the development of the reaction mixture's absorbance over the course of the polymerisation process, an UV/Vis spectrum of purified PMTC as well as of the separated oligomeric residue was measured, utilising a few drops of viscous PMTC and oligo-PMTC dissolved in distilled THF (**Figure S11**).

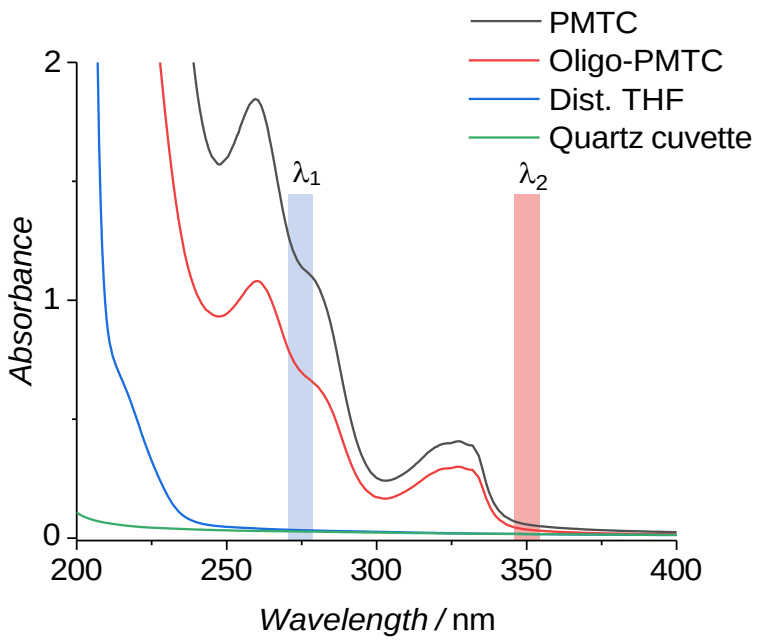

***Figure S11**. UV/Vis spectra of PMTC and its oligomeric supernatant after purification in distilled THF together with pure solvent and blank quartz cuvette.*

2.8 Computational studies

For the computational evaluation of the proposed delocalised tertiary radical **I**, two reference structures were modelled and theoretically assessed with regards to bong length, bond order, and charge (**Figure 2**+**Figure S12**).

A

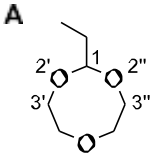

Bond	*Bond length / pm*	Bond order	Atom	Charge
C1-O2'	142.6	0.958	C1	0.182
C1-O2''	143.1	0.968		
O2'-O3'	143.4	0.956	O2'	-0.209
O2''-C3''	143.5	0.968	O2''	-0.206
			C3'	0.036
			C3''	0.029

B

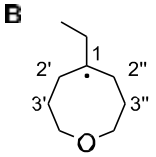

Bond	*Bond length / pm*	Bond order	Atom	Spin population	Charge
C1-C2'	152.9	0.985	C1	1.196	0.023
C1-C2''	152.9	0.985			
C2'-C3'	155.0	0.983	C2'	-0.148	-0.054
C2''-C3''	154.3	0.991	C2''	-0.148	-0.050
			C3'	0.056	-0.047
			C3''	0.025	-0.055

***Figure S12**. Reference molecules: (A) cyclic intermediate without tertiary radical at central C1 and (B) cyclic tertiary radical where α-oxygens 2' and 2'' were substituted with carbons together with their corresponding computational values determined via STO-6G as basis set.*

A comprehensive overview of all applied basis sets for the calculation of the transition moment of radical **I** is depicted in the following (**Table S6**).

Table S6. *Overview of all utilised basis set and their corresponding calculated transition moments.*

Basis set	*Transition moment /* nm
STO-6G	473.3
6-31G	312.3
6-31G*	310.7
6-31G**	311.5
SPK-ADZP	310.7
KTZV	312.3
KTZVP	310.7
KTZVPP	310.7
PCseg-0	306.9
PCseg-1	305.4
PCseg-2	305.4
APCseg-0	315.5
APCseg-1	306.9
CCD	310.7
CCT	311.5
ACCD	311.5

3 References

1. F. Mehner, T. Meissner, A. Seifert, A. Lederer and J. Gaitzsch, Kinetic studies on the radical ring-opening polymerization of 2-methylene-1,3,6-trioxocane, *Journal of Polymer Science*, 2023, **61**, 1882-1892.
2. F. Mehner, M. Geisler, K. Arnhold, H. Komber and J. Gaitzsch, Structure–Property Relationships in Polyesters from UV-Initiated Radical Ring-Opening Polymerization of 2-Methylene-1,3-dioxepane (MDO), *ACS Applied Polymer Materials*, 2022, **4**, 7891-7902.
3. R. S. Mulliken, Electronic Population Analysis on LCAO–MO Molecular Wave Functions. I, *The Journal of Chemical Physics*, 1955, **23**, 1833-1840.
4. P.-O. Löwdin, in *Adv. Quantum Chem.*, ed. P.-O. Löwdin, Academic Press, 1970, vol. 5, pp. 185-199.
5. M. W. Schmidt, K. K. Baldridge, J. A. Boatz, S. T. Elbert, M. S. Gordon, J. H. Jensen, S. Koseki, N. Matsunaga, K. A. Nguyen, S. Su, T. L. Windus, M. Dupuis and J. A. Montgomery Jr, General atomic and molecular electronic structure system, *J. Comput. Chem.*, 1993, **14**, 1347-1363.
6. B. P. Pritchard, D. Altarawy, B. Didier, T. D. Gibson and T. L. Windus, New Basis Set Exchange: An Open, Up-to-Date Resource for the Molecular Sciences Community, *J. Chem. Inf. Model.*, 2019, **59**, 4814-4820.
7. T. Noro, M. Sekiya and T. Koga, Segmented contracted basis sets for atoms H through Xe: Sapporo-(DK)-nZP sets (n = D, T, Q), *Theor. Chem. Acc.*, 2012, **131**, 1124.
8. F. Jensen, Unifying General and Segmented Contracted Basis Sets. Segmented Polarization Consistent Basis Sets, *J. Chem. Theory Comput.*, 2014, **10**, 1074-1085.
9. A. Schäfer, H. Horn and R. Ahlrichs, Fully optimized contracted Gaussian basis sets for atoms Li to Kr, *The Journal of Chemical Physics*, 1992, **97**, 2571-2577.
10. A. Schäfer, C. Huber and R. Ahlrichs, Fully optimized contracted Gaussian basis sets of triple zeta valence quality for atoms Li to Kr, *The Journal of Chemical Physics*, 1994, **100**, 5829-5835.
11. T. H. Dunning, P. J. Hay and H. F. Schaefer, Methods of electronic structure theory, *Modern theoretical chemistry*, 1977, **3**, 1--28.
12. I. M. Irshadeen, S. L. Walden, M. Wegener, V. X. Truong, H. Frisch, J. P. Blinco and C. Barner-Kowollik, Action Plots in Action: In-Depth Insights into Photochemical Reactivity, *J. Am. Chem. Soc.*, 2021, **143**, 21113-21126.
13. J. P. Menzel, B. B. Noble, A. Lauer, M. L. Coote, J. P. Blinco and C. Barner-Kowollik, Wavelength Dependence of Light-Induced Cycloadditions, *J. Am. Chem. Soc.*, 2017, **139**, 15812-15820.